

## RESEARCH

# A digital subtraction radiography scheme based on automatic multiresolution registration

EI Zacharaki<sup>1</sup>, GK Matsopoulos\*<sup>1</sup>, PA Asvestas<sup>1</sup>, KS Nikita<sup>1</sup>, K Gröndahl<sup>2</sup> and H-G Gröndahl<sup>2</sup>

<sup>1</sup>Institute of Communication and Computer Systems, National Technical University of Athens, Athens, Greece; <sup>2</sup>Department of Oral and Maxillofacial Radiology, Faculty of Odontology, The Sahlgrenska Academy at Göteborg University, Göteborg, Sweden

**Objectives:** To establish a digital subtraction radiography scheme for aligning clinical *in vivo* radiographs based on the implementations of an automatic geometric registration method and a contrast correction technique.

**Methods:** Thirty-five pairs of *in vivo* dental radiographs from four clinical studies were used in this work. First, each image pair was automatically aligned by applying a multiresolution registration strategy using the affine transformation followed by the implementation of the projective transformation at full resolution. Then, a contrast correction technique was applied in order to produce subtraction radiographs and fused images for further clinical evaluation. The performance of the proposed registration method was assessed against a manual method based on the projective transformation.

**Results:** The qualitative assessment of the experiments based on visual inspection has shown advantageous performance of the proposed automatic registration method against the manual method. Furthermore, the quantitative analysis showed statistical difference in terms of the root mean square (RMS) error estimated over the whole images and specific regions of interest.

**Conclusions:** The proposed automatic geometric registration method is capable of aligning radiographs acquired with or without rigorous *a priori* standardization. The methodology is pixel-based and does not require the application of any segmentation process prior to alignment. The employed projective transformation provides a reliable model for registering intraoral radiographs. The implemented contrast correction technique sequentially applied provides subtraction radiographs and fused images for clinical evaluation regarding the evolution of a disease or the response to a therapeutic scheme.

*Dentomaxillofacial Radiology* (2004) 33, 379–390. doi: 10.1259/dmfr/21571843

**Keywords:** subtraction radiography, image registration, fusion, projective transformation, contrast correction

## Introduction

The diagnostic problem of comparing radiographic images over time lies primarily in the identification of the image features that are solely related with the progression or regression of a particular disease. It is common knowledge that visual comparison of paired radiographs corresponding to different time instances creates confusion, mainly due to the presence of structured noise resulting from anatomical details projected over the area of radiographic change.<sup>1</sup> Digital subtraction radiography is a computer-aided radiographic analysis tool that can be used for the

detection and visualization of early changes in periodontal disease<sup>2</sup> or around implants<sup>3</sup> as well as for the monitoring and evaluation of therapeutic procedures<sup>4</sup> or agents in clinical trials.<sup>5</sup>

Experts commonly identify changes in the bone structure supporting the teeth by comparing radiographs acquired over a short or long period of time. Studies have shown that the level of standardization of the projection geometry greatly influences the performance of the subtraction radiography. Two sources of errors in projection geometry that contribute to misregistration are misalignment of object to source and misalignment of object and film.<sup>6</sup> To minimize these projection errors, the relative location and orientation of the X-ray source, the

\*Correspondence to: George K Matsopoulos, 9, Iroon Polytechniou str, Zografos, 15780, Athens, Greece; E-mail: [gmatso@esd.ece.ntua.gr](mailto:gmatso@esd.ece.ntua.gr)  
Received 11 February 2004; revised 30 August 2004; accepted 3 October 2004

dental area of interest and the film (or X-ray sensor) must be maintained at different examinations. However, this is only the first step towards successful subtraction radiography. Since the reproducibility of imaging geometry cannot be guaranteed, a second step of spatial registration is required before subtraction based on image processing.

Lehmann *et al* presented a comprehensive review of techniques according to the aforementioned steps that may be applied towards successful subtraction radiography.<sup>7</sup> Concerning the projection geometry stabilization, external mechanical devices have been used to reduce all possible projection errors.<sup>8–11</sup> The development of image processing techniques allows the sequential reconstruction of the acquired image geometry and the contrast correction of the radiographs before subtraction. Most investigators use manual alignment according to which anatomical landmarks are initially marked in both radiographic images by experienced observers and then used to fit a transformation model according to a measure of match.<sup>12,13</sup> Recently, automatic registration techniques have also been introduced in the literature. Ettinger *et al*<sup>11</sup> proposed the bilinear warping of radiographic pairs based on the automatic segmentation of cemento-enamel junctions and edge contours using the gradient operator. Similarly, an automatic registration method has been proposed based on the segmentation of the two radiographic images, using a  $3 \times 3$  Sobel operator, and the application of the affine transformation.<sup>14</sup> Most of these image processing techniques can recover projection errors occurring when the sensor translates or rotates relative to the object or when the object rotates around the  $z$ -axis relative to the source. Projection errors due to rotation of the object horizontally or vertically relative to the source are irreversible and they cannot be controlled in *in vivo* studies, *i.e.* clinical radiographs acquired over long periods of time. The performance of registration algorithms in the presence of irreversible projection errors can be assessed on *in vitro* data with a known relative location of the source, object and detector.<sup>6,13,15</sup>

In the present study, a registration and fusion scheme is proposed for the creation of subtraction radiographic images. The scheme has been tested *in vivo* in intraoral radiographs acquired from different clinical studies over a short or long period of time with and without rigorous *a priori* standardization. Although special attempt has been made to keep the acquisition environment constant, inevitably projection errors have occurred in some cases.

Thus, the purpose of the paper is two-fold: (a) the establishment of a generalized automatic registration/fusion scheme for subtraction radiography applied to *in vivo* radiographic images; and (b) the assessment of its performance against the widely used manual approach based on the projective transformation.

## Materials and methods

### *Experimental procedure*

The radiographs used in this work were acquired using a dental X-ray machine and selected from four clinical

studies in order to test the suitability of the developed automatic registration scheme for the evaluation of the progression of different diseases.

The first clinical study aimed to evaluate the effect of subgingival antimicrobial irrigation to patients with periodontal bone loss.<sup>16</sup> Seven patients with moderate to severe periodontal bone loss were selected providing seven registration sets. The second study refers to patients with single implants (Astra Tech AB, Mölndal, Sweden) examined at different occasions to follow-up the marginal bone support at the implants over time. The same study includes images from patients with Brånemark implants (NobelBiocare AB, Göteborg, Sweden). Fifteen registration pairs were provided for alignment by this study. The third study was performed on dogs in order to compare marginal bone level measurements around implants with varying degree of bone loss.<sup>17</sup> The bone loss was initiated by connecting abutments on the installed implants and placing cotton ligatures. Radiographs from the right side of one dog taken at six occasions have provided five registration pairs (R1–R5). Three more registration pairs have been obtained after the removal of the abutments and the submerging of the implants (R6–R8). Finally, five bite-wing image pairs have been selected at random from a fourth clinical study. Hence, in the present work, the total number of radiographs from the aforementioned clinical studies added up to 35 pairs.

In the first clinical study the radiographs were taken by means of a device modified after one described by Rosling *et al*.<sup>18</sup> Consequently, the radiographs provided by this study were rigorously standardized *a priori*. In the other studies radiographs, with the film kept parallel and the X-ray beam perpendicular to the implant, were taken using an individually fabricated filmholder. The filmholder was attached to the occlusal surface of the suprastructure or to a reference implant with impression coping, using an impression material. Since there was no mechanical connection to the X-ray machine, the data from these studies may have contained small reversible and irreversible projection errors. Some radiographs were acquired in a time period of 1–3 months, whereas others within a time period of more than 6 months. Taking into account the projection differences between the examinations, the possible shrinkage in the impression material, the problems to place the filmholder in exact position even if there are impressions from the teeth, the difference that might occur in the relation between the filmholder and the aiming device of the X-ray machine, it could be assumed that the projection difference was within the range of 1–5 degrees with all possible combinations in all planes.

All radiographs were digitized with a flatscanner (Agfa Arcus II) producing 8-bit grey scale image files. Each image acquired initially in every case formed the reference (baseline) image and was registered against radiographs obtained at subsequent times. The data have included white background representing regions outside the film limits. Moreover, some radiographs have included parts of the filmholder or impression material. This information is unnecessary for the purpose of the present work and its presence may disorientate the proposed automatic

registration procedure since it participates in the matching process. Therefore, in these cases, the spatial match was restricted to cropped images excluding the undesired parts. The size of the cropped radiographs ranged from  $608 \times 502$  pixels to  $1628 \times 1288$  pixels. If the baseline radiograph was registered with more than one subsequent radiograph, all of them were cropped starting from the same pixel coordinates (upper left image corner). By inference, the image cropping should not be considered as a pre-registration step as it does not introduce any image displacement. The cropped subsequent radiograph was then registered by applying both the geometric registration and contrast correction methods.

*The proposed digital subtraction radiography scheme*

For the creation of digital subtraction radiographic images, a registration/fusion scheme is proposed as illustrated in Figure 1. It is comprised of two main processes: the geometric registration and the contrast correction techniques. The differences between the reference ( $I_R$ ) and the subsequent ( $I_F$ ) radiograph can be considered as the effect of three mechanisms: (a) local anatomical deformations due to progression or regression of a disease; (b) geometric transformation due to projection errors (reversible and irreversible<sup>6,12</sup>); and (c) intensity transformation due to non-identical exposure or film processing parameters.<sup>19</sup> The demonstration of the anatomical dissimilarities can be achieved if the other two mechanisms are eliminated. Nevertheless, there is no inverse geometric transformation eliminating irreversible projection errors. An inverse geometric transformation ( $T_{geom}$ ) is sought to eliminate the reversible projection errors even under the presence of irreversible projection errors producing the aligned image ( $I_{tr}$ ). Furthermore, an inverse intensity transformation ( $T_{grey}$ ) is searched for to correct the contrast of the radiographs<sup>7,20</sup> creating the geometric transformed and contrast corrected image ( $I_{gtr}$ ).

In the following sections the steps of the digital subtraction radiography scheme are presented in detail.

*The proposed automatic geometric registration method*

The automatic registration method is based on a novel assembly of image processing techniques, which ultimately offer increased degree of automation by minimizing the need for user intervention. The method is pixel-based, i.e. it operates on the image's grey levels without any requirement for the application of a segmentation process prior to registration.<sup>21</sup> The proposed algorithm consists of two steps. In the first step, a coarse registration of the two

radiographs is obtained by calculating the parameters of an affine transformation. For the calculation of these parameters, a multiresolution strategy<sup>22,23</sup> is employed. In the second step, the registration is refined by implementing the projective transformation. The projective transformation parameters are calculated using, as starting estimates, the previously obtained affine transformation parameters. The automatic registration procedure is illustrated in Figure 2 and is explained in the following.

*Step 1* Alignment of the two radiographs is accomplished by transforming the image to be registered using a two-dimensional (2D) affine transformation:

$$\begin{pmatrix} x' \\ y' \\ 1 \end{pmatrix} = \begin{pmatrix} a_1 & a_2 & dx \\ a_3 & a_4 & dy \\ 0 & 0 & 1 \end{pmatrix} \begin{pmatrix} x \\ y \\ 1 \end{pmatrix} \quad (1)$$

where  $a_i$ ,  $i = 1..4$ , are the parameters of the affine transformation defining the rotation and the scaling and  $dx$ ,  $dy$  are the parameters defining the translation in the  $x$ - and  $y$ -direction, respectively. The parameters of the affine transformation are calculated automatically by maximizing a similarity criterion between the reference image  $I_R(x, y)$  and the image to be registered  $I_F(x, y)$ . For intramodal image registration, the normalized cross-correlation (CC) coefficient is a suitable matching criterion, which is defined as follows:

$$CC = \frac{\sum_{x,y} [I_F(x, y) - \bar{I}_F][I_R(T_A(x, y)) - \bar{I}_R]}{\sqrt{\sum_{x,y} [I_F(x, y) - \bar{I}_F]^2} \sqrt{\sum_{x,y} [I_R(T_A(x, y)) - \bar{I}_R]^2}} \quad (2)$$

where  $\bar{I}_F$  and  $\bar{I}_R$  are the corresponding mean values of the images.

The multidimensional maximization of the selected similarity measure is achieved by introducing a multi-resolution scheme applied from coarse to fine levels. According to this iteration strategy, the affine parameters are calculated at each resolution level by maximizing the normalized cross-correlation coefficient of the subsampled images. The subsampled images are produced by applying a weighting function. According to the methodology applied, a subsampled image  $I_{sf}$  of the original  $I$  using

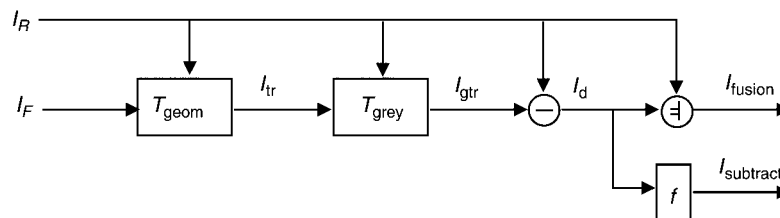


**Figure 1** Digital subtraction radiography scheme.  $T_{geom}$  represents the geometric registration (automatic or manual) and  $T_{grey}$  the contrast correction. The minus operator denotes the difference, the operator  $=$  models the fusion process and  $f(x) = (x + 255)/2$

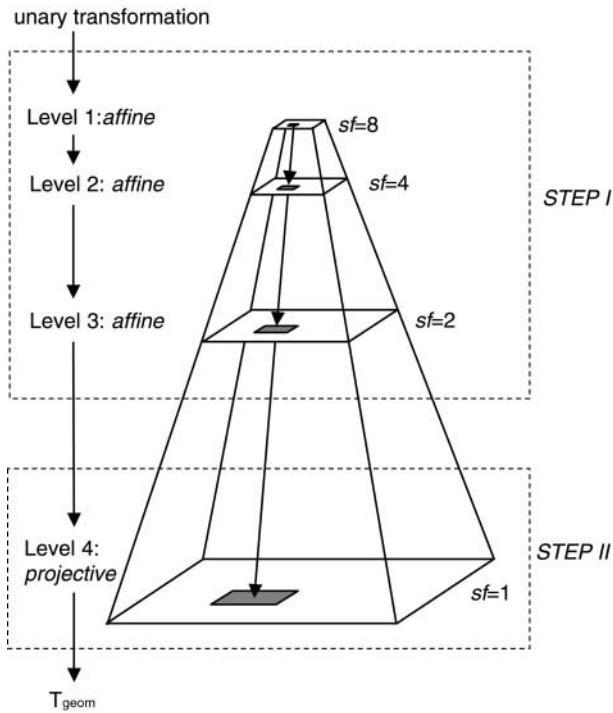


**Figure 2** Schematic representation of the proposed automatic geometric registration procedure.  $T_{geom}$  denotes the final geometric transformation and  $sf$  the sampling factor

the same sampling factor  $sf$  in the  $x$  and  $y$  coordinate dimensions is obtained by the following equation:

$$I_{sf}(r_i) = \frac{\sum_{j=1}^{sf \times sf} w_j I(sf \cdot r_i + \delta r_j)}{\sum_{j=1}^{sf \times sf} w_j}, \quad (3)$$

$$w_j = \begin{cases} 1.5, & \delta r_j = 0 \\ \frac{1}{\|\delta r_j\|}, & \delta r_j \neq 0 \end{cases}$$

where  $\delta r = (\delta x, \delta y)$ ,  $0 \leq \delta x, \delta y < sf$ .

The maximization of the similarity measure is performed with the application of a local optimization technique. Optimization starts at the coarsest level with parameters  $a_1 = a_4 = 1$  and all other parameters set to zero (unary transformation). The obtained parameters are used as the initial solution for the next resolution level. Starting the optimization procedure from the coarse level, the possibility of getting trapped into some local optima is reduced since the matching criterion employed is smoothed. After convergence, switching to finer levels enhances the accuracy.<sup>22</sup> A subsequent benefit of the multiresolution strategy is that, if the optimum at a lower-resolution level is close to the optimum at the next higher-resolution level, most of the iterations will be very probably carried out at the low level, where the amount of data is small.<sup>23</sup> If the sampling factors along the  $x$ - and  $y$ -coordinate dimensions are denoted as  $sf_x$  and

$sf_y$ , subsampling results in a speed-up by a factor  $sf_x \times sf_y$  in the evaluation of the similarity measure. If the lower and the higher-resolution level do not converge to the same optimum, then the evaluations at low resolution are useless and time consuming. In order to avoid misconvergence and increase registration robustness, the difference between the image resolutions from level to level should be kept small. Thus, a three-level multiresolution strategy with  $sf_x = sf_y = 8, 4, 2$  is finally employed. Optimization at full resolution ( $sf_x = sf_y = 1$ ) is performed at Step II.

The search strategy applies a local optimization technique namely the Downhill Simplex Method (DSM).<sup>24</sup> According to Maes et al.,<sup>23</sup> DSM is an optimization method often employed owing to its simplicity and suitability for solving similar multiresolution optimization problems. The length scale of the disturbance vectors is quite high at the first level ( $sf_x = sf_y = 8$ ) in order to render the registration method applicable in the case of large transformations as well. However, after each optimization convergence, the length scale of the disturbance vectors is reduced so as to speed up the execution. The fractional convergence tolerance in the function value was kept at  $10^{-4}$  at all resolution levels.

*Step II* According to Lehmann et al.<sup>12</sup> and Ostuni et al.,<sup>25</sup> intraoral radiography is approximated by a perspective projection. The 2D projective transformation is given by the following equation:

$$\begin{pmatrix} u \\ v \\ w \end{pmatrix} = \begin{pmatrix} a_1 & a_2 & dx \\ a_3 & a_4 & dy \\ a_5 & a_6 & 1 \end{pmatrix} \begin{pmatrix} x \\ y \\ 1 \end{pmatrix}, \quad \begin{pmatrix} x' \\ y' \end{pmatrix} = \begin{pmatrix} u/w \\ v/w \end{pmatrix} \quad (4)$$

where  $w$  represents the extra homogeneous coordinate and  $u$  and  $v$  are dummy variables. The projective transformation introduces two more variables than the affine transformation,  $a_5$  and  $a_6$ . Thus, a total of eight parameters are required to fully define the projective transformation. It can be noticed that the affine transformation (Equation 1) can be seen as a special case of perspective projection with  $a_5 = a_6 = 0$ . In the proposed registration algorithm, the optimal values of the projective transformation parameters are obtained by maximizing the normalized cross-correlation coefficient of the full resolution images and applying the DSM, as an optimization method. The initial starting point for the optimization at full resolution is the vector of the affine parameters, as estimated in the previous step together with  $a_5$  and  $a_6$  set to zero.

#### The manual approach

In the case of dental X-ray images, which exhibit strong edges, a manual approach to the image registration problem can also be implemented. Homologous pairs of points are placed interactively on the images to be registered by the expert by means of appropriate software. In the particular implementation, a graphical user interface for image input and display has been developed. By clicking with the mouse on the reference and the unregistered image, a data file is created which includes

the landmark coordinates and constitutes the input file for the manual registration algorithm. The corresponding landmarks are aligned by applying the projective transformation. Four pairs of landmarks are sufficient to compute the parameters of the projective transformation. In our approach, a number of nine to 16 pairs of points is used, in order to balance out random errors and achieve robustness of the transformation. During the evaluation, the parameters of the projective transformation are calculated by applying the least squares minimization method<sup>26</sup> in conjunction with singular value decomposition (SVD), since the number of user defined landmarks is greater than the number of independent parameters of the projective transformation.

#### Contrast correction algorithm

Contrast correction is performed subsequent to geometric registration in order to correct differences in the intensity of the images. The grey level transformation is based on the non-parametric method proposed by Ruttimann et al<sup>20</sup> and is derived directly from the histograms of the baseline and the geometric transformed image calculated within the region of overlap.

#### Subtraction and pseudocolouring

After the geometrically aligned and contrast corrected image,  $I_{gtr}$ , is produced, subtraction radiography is then performed (see Figure 1). Initially, the difference image ( $I_d$ ) is calculated by subtracting the grey values of the reference image from the grey values of the aligned and contrast corrected image in the region of overlap, and set to zero outside. The difference image should ideally be non-zero only in areas where changes in structure have occurred. Then, the subtraction image ( $I_{subtract}$ ) is obtained as a linear function of the difference image<sup>6</sup> according to the following equation:

$$I_{subtract}(x, y) = (I_d(x, y) + 255)/2 \quad (5)$$

The subtraction image represents bone gain or bone loss with light or dark areas, respectively.

The anatomical location of the disease is visualized by superimposing the subtraction image to the reference image, according to the following masking process:

$$I_{fusion}(x, y) = \left\{ \begin{array}{ll} I_R(x, y), & \text{if } |I_d(x, y)| < \text{threshold} \\ \infty |I_d(x, y)|, & \text{if } |I_d(x, y)| \geq \text{threshold} \end{array} \right\} \quad (6)$$

where  $I_{fusion}$  is the fused image and the symbol  $\infty$  denotes the intensity which is displayed in a colour scale. For this purpose, a hot body colour map is created to indicate the size of the difference. The combination of a grey scale (256 grey levels) and a colour scale in the same image helps in enhancing the visibility of the fused image. A threshold defined by the user is applied in order to illustrate areas of significant change, thus distinguishing noise from any pathological dissimilarity. The threshold can be selected after an iterative inspection of the fusion result as a trade-off between minimizing noise and preserving the depiction of any pathological change. The fusion images should not

be used for the performance of measurements (e.g. bone level measurements) because of their variability caused by the threshold selection. Any measurements should be performed on the subtraction images.

#### Evaluation of performance

The image registration accuracy can be visually assessed by inspecting the subtraction image or the fused image. Furthermore, the registration accuracy can be quantitatively measured using the root mean square difference (RMS)<sup>14</sup> between the reference and the (geometric and intensity) aligned image. The RMS difference is calculated as follows:

$$RMS = \sqrt{\frac{\sum_{i=1}^N (I_R(\bar{r}_i) - I_{gtr}(\bar{r}_i))^2}{N}} \quad (7)$$

where the sum is calculated only over the  $N$  pixels belonging to the region of overlap of the reference ( $I_R$ ) and the aligned image ( $I_{gtr}$ ). Generally, for the same image pair, the smaller the RMS error the better the registration achieved. The RMS error is also calculated on specific regions of interest (ROIs) located by an experienced dentist.

## Results

#### Qualitative analysis

Figure 3 shows the digital subtraction results for a pair of radiographs selected from the first study. Figures 3a and b show the reference and the subsequent radiograph. Figures 3c and d show the corresponding cropped radiograph applied in the registration process. The registered radiograph is shown in Figure 3e. In order to visually assess the proposed automatic registration method, the edges of the registered image were detected by applying a  $3 \times 3$  Sobel gradient filter<sup>27</sup> and superimposed to the baseline image, as illustrated in Figure 3f, which reveals successful registration. The subtraction image is also created and displayed in Figure 3g. Finally, the information of the subtraction image is fused with the baseline image. The fused image (Figure 3h) was created by applying a threshold of 20 grey levels. The subtraction image confirms that the vertical osseous defect at the mesial surface of the first molar has become more sclerotic after successful therapy. The minimum projection errors are due to the high standardization upon acquisition of the radiographs of the first study.

In Figures 4 and 5, two radiography pairs of the second study are used to visually compare the automatic registration method against the manual one. Even though image cropping is not necessary during manual registration, for consistency of comparisons (i.e. when calculating the RMS error), cropped images were used for both the automatic registration method and the manual approach. Figures 4a and b show an example of the placement of anatomical landmarks (small white crosses) on the

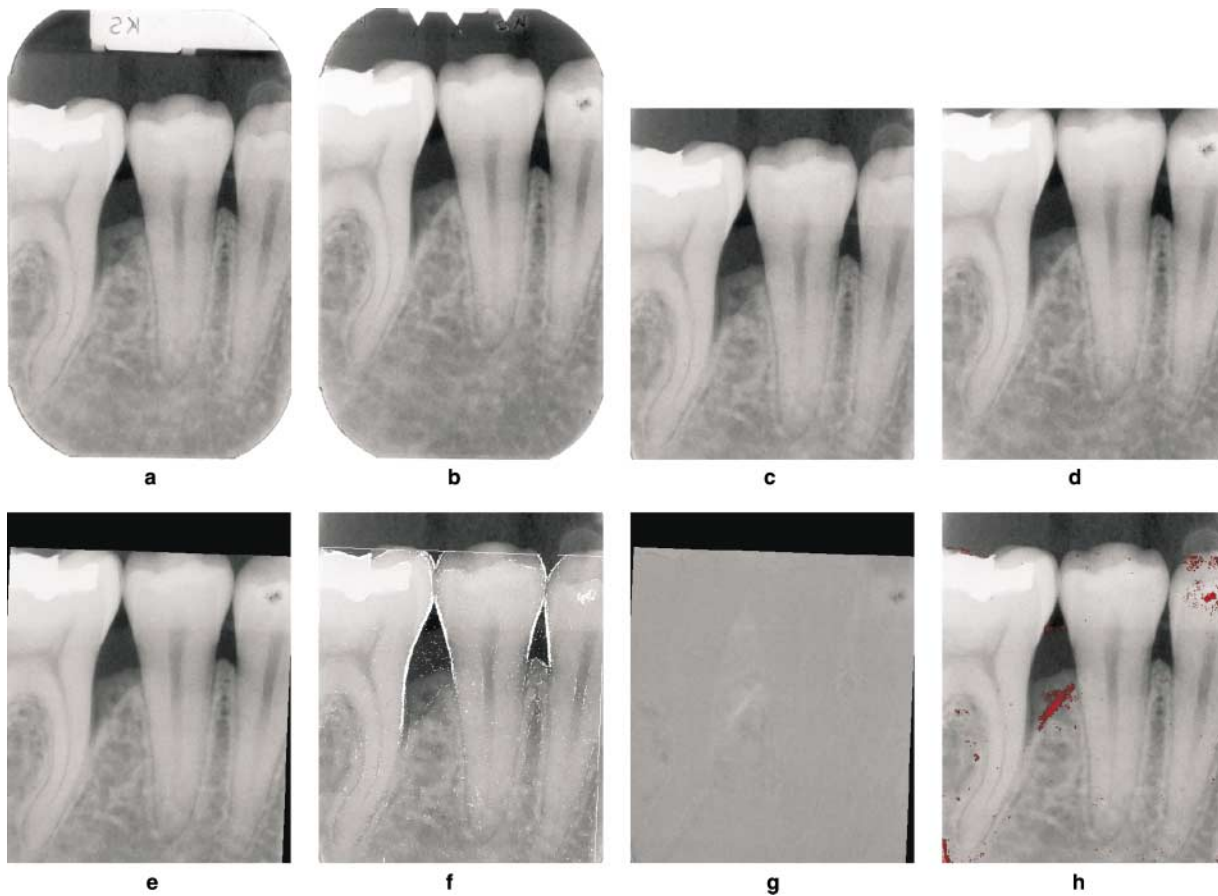


**Figure 3** The automatic registration method. (a) The original baseline radiograph. (b) The radiograph to be registered. (c, d) The cropped images of (a) and (b), respectively. (e) The registered radiograph after the application of the automatic geometric registration and contrast correction methods. (f) Superposition of the edges of the registered radiograph (e) on the baseline image (c). (g) The subtraction image. (h) The fused image

reference and the subsequent radiograph. The landmarks are used in order to calculate the manual projective transformation. The result of the manual registration approach is shown in Figure 4c. The registered image resulting by means of the manual registration approach is compared against the proposed automatic registration method. The result of the automatic registration method is displayed in Figure 4d. White arrows are drawn on the registered images to indicate local misalignments. Similar results are also presented in Figure 5.

The visual assessment of the results presented in Figures 4 and 5 reveals that both methods generally could be used for registering radiographic images. However, careful inspection of the results reveals that the automatic registration method outperforms the manual one. It can be noticed that the manual method performs well locally in the areas where the expert places points of correspondence. These landmarks have been placed on line intersections and around the implants since these areas determine the follow-up of the marginal bone support. As a consequence, the manual registration may fail within the rest of the image.

Finally, the example in Figure 6 refers to the third study series aiming to compare marginal bone level measurements around implants with varying degree of bone loss.<sup>17</sup> R2 indicates the time immediately before breakdown of the

marginal bone support, R4 the middle of the breakdown period and R7 the maximum breakdown. In Figure 6 the baseline image (R1) is displayed along with the fused images at the times of the breakdown period R3, R4, R5 and R6. The proposed automatic geometric registration method was applied. Only differences above a threshold level of 35 grey values are highlighted in pseudocolour. They correspond to the progression of the marginal bone loss at different periods. It can be noticed that bone loss is apparent in areas around implants. Nevertheless, there are regions within the upper part of the radiograph illustrating the impression material where differences are also recorded. A possible explanation of the observed differences can be that the impression coping was not seated correctly. Hence, a shift in projection geometry had occurred. Another explanation might be that the dog's lower lip was kept differently during the exposure.

#### *Quantitative analysis*

A quantitative analysis has also been performed in order to assess the performance of the proposed automatic registration method against the manual one. The comparison of the two methods was based on the RMS error between the reference and the aligned image. Contrast correction was applied to both automatically and manually aligned images

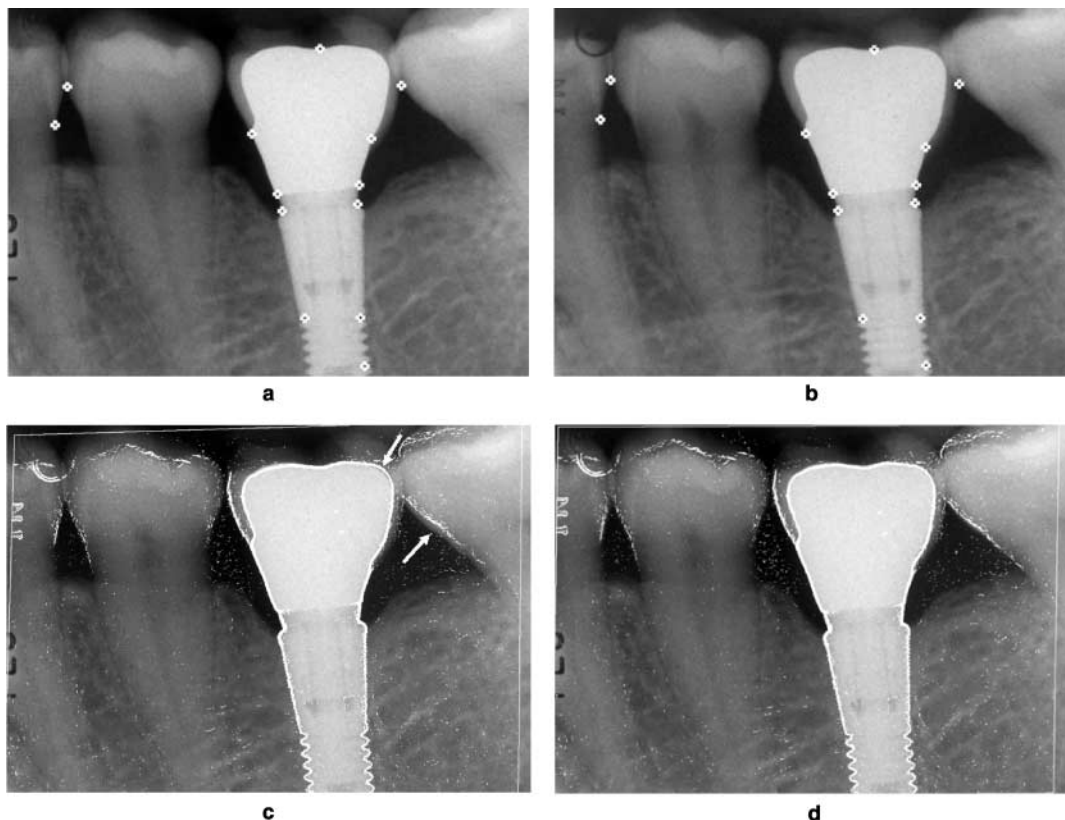


**Figure 4** Manual registration is performed by placing 13 landmarks (marked with white crosses) on the reference (a) and the subsequent (b) radiograph. The edges of (c) the manually and (d) the automatically registered radiograph are superimposed to the reference image. White arrows indicate local misalignments

in the same fashion. The results are shown in Table 1. As the manual registration accuracy depends on the number of landmarks (NL), Table 1 lists the NL for all pairs of radiographs used. The mean RMS value and the standard deviation (SD) of the RMS value for the 35

registration pairs were calculated for both the automatic and the manual method. The RMS error of the manual registration method represents averaged values over five executions by the same observer to compensate for the operator variability of the manual method.

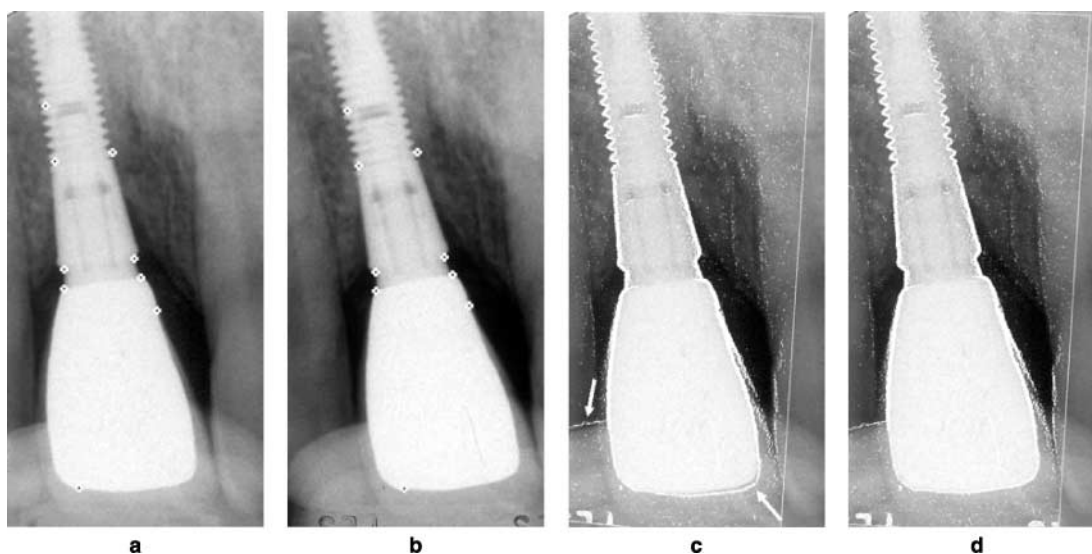


**Figure 5** Manual registration is performed by placing nine landmarks (marked with white crosses) on (a) the reference and (b) the subsequent radiograph. The edges of (c) the manually and (d) the automatically registered radiograph are superimposed to the reference image. Again, white arrows indicate local misalignments

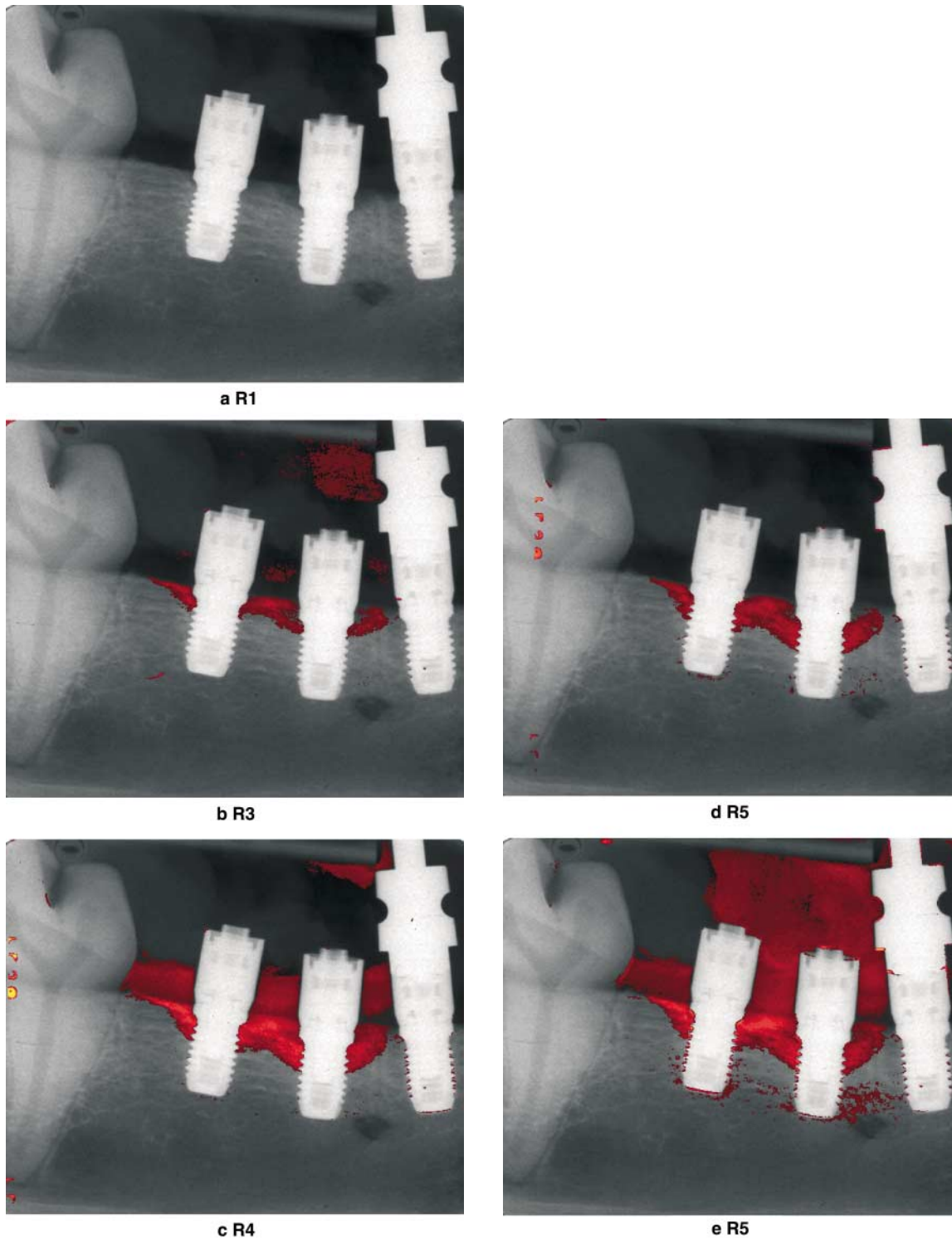


**Figure 6** The baseline radiograph (R1) fused each time with a subsequent radiograph (R3–R6). The colour scale illustrates differences that are higher than 35 grey levels

From Table 1, it is evident that the proposed automatic registration method for all radiographic pairs outperforms the manual method in terms of the RMS error estimated over the whole images. However, these estimated RMS errors are not always representative for the registration accuracy, mainly due to the anatomical changes that are

counted in the estimation of the RMS value. Since beam parallelism is generally not preserved in radiography, an image receptor not perpendicular to the central beam induces distortions due to objects lying at different distance from the focus. In order to evaluate the accuracy of the two registration methods, ROIs (same in both the automatically

**Table 1** Automatic versus manual geometric registration in terms of the root mean square (RMS) error

Pair No.	NL	Manual method		Automatic method	
		RMS (whole images)	RMS (selected ROIs)	RMS (whole images)	RMS (selected ROIs)
01	11	16.3	7.0	11.6	7.1
02	12	10.1	10.5	9.2	8.9
03	11	9.1	7.5	8.5	6.8
04	11	7.9	8.9	7.3	7.9
05	11	7.4	7.2	7.3	6.9
06	13	11.9	10.9	11.5	10.1
07	9	18.8	13.3	18.6	13.1
08	16	10.6	8.9	10.4	8.8
09	13	9.6	8.4	9.3	8.5
10	12	13.8	11.6	13.6	11.6
11	14	13.8	18.3	12.7	16.0
12	9	12.2	11.2	11.9	10.6
13	16	17.8	14.9	13.1	13.5
14	16	9.4	9.1	9.2	8.8
15	16	14.1	13.1	13.8	12.6
16	16	14.9	21.2	14.1	19.0
17	16	19.3	13.3	16.0	12.2
18	15	13.6	9.4	11.9	9.0
19	15	10.8	8.8	9.8	8.6
20	15	13.0	10.2	12.6	10.1
21	15	9.2	9.2	8.2	8.3
22	12	17.2	21.0	9.2	13.4
23	13	8.6	9.0	8.0	6.9
24	12	27.5	37.3	21.0	28.3
25	16	13.1	9.2	12.7	9.1
26	12	23.1	12.9	22.6	12.0
27	15	17.1	20.5	16.8	20.5
28	14	15.0	17.9	12.7	16.2
29	13	13.4	17.0	12.0	14.3
30	16	14.0	16.7	12.1	10.5
31	16	12.2	15.9	12.0	15.3
32	11	41.9	20.8	28.1	21.1
33	11	41.3	25.5	38.3	23.5
34	14	16.8	12.2	15.2	10.3
35	12	9.3	9.3	7.6	6.8
Mean value ± SD		15.260 ± 7.866	13.660 ± 6.318	13.397 ± 6.247	12.189 ± 5.153

ROI, region of interest; SD, standard deviation; NL, number of landmarks

and manually registered images) were selected by an experienced dentist. Only stable structures such as the crown of the teeth or implants were included whereas areas with anatomical changes such as the marginal bone were omitted. The RMS error estimated on these ROIs is an improved local measure of the alignment accuracy less dependent on the overall distortions. Practically, the smaller the RMS value estimated, the better the registration achieved. The RMS values estimated over these ROIs are also shown in Table 1. It can be concluded that the proposed automatic registration method outperforms for the majority of radiographic pairs included in this study (30/35) in terms of the RMS values estimated over specific ROIs. For the other five pairs, the performance of the manual method is superior for only three pairs whereas for the remaining two pairs, the performance is equivalent for both methods. In addition, the performance of the two geometric registration methods was assessed through visual inspection of all subtraction images by an experienced dentist. The findings were in accordance with the estimated RMS values.

The statistical difference between the RMS value of the subtraction image produced by the automatic (RMS<sub>AUTO</sub>) and the manual (RMS<sub>MAN</sub>) registration method estimated

over the whole images and on the ROIs was also assessed. In Figure 7, the Bland–Altman plots<sup>28</sup> of the RMS error of the two methods under comparison are shown. The Bland–Altman plots illustrate the difference between a pair of measurements (RMS<sub>MAN</sub> – RMS<sub>AUTO</sub>) against their average value (RMS<sub>MAN</sub> + RMS<sub>AUTO</sub>)/2. The plots demonstrate that the manual method tends to give RMS values that are higher than the proposed automatic method both for the whole images and the selected ROIs. Additionally, statistical analysis was conducted by means of the paired *t*-test under the null hypothesis that the two methods did not differ as per the RMS value. The alternative hypothesis was that the RMS error for the automatic registration method is smaller than that for the manual one. For both cases, whole images and ROIs, the null hypothesis was rejected (*P* < 0.01) in favour of the alternative hypothesis.

## Discussion

The aim of the present paper is to introduce an improved digital subtraction radiography scheme based on an automatic geometric registration method and a contrast correction method for aligning digital radiographs

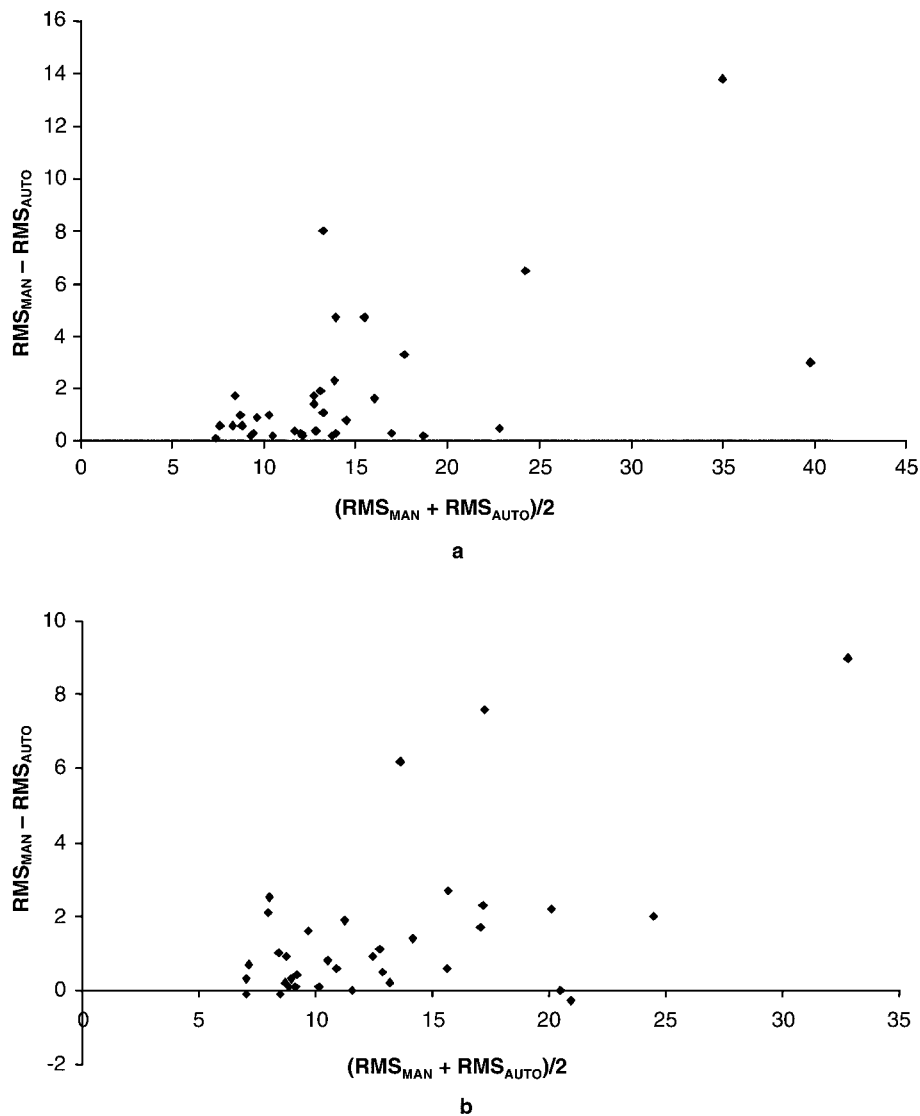


**Figure 7** Bland–Altman plot of the root mean square (RMS) error of the two registration methods under comparison: (a) for whole images; (b) for selected regions of interest (ROIs)

acquired with or without rigorous *a priori* standardization. The automatic geometric registration method was developed in order to overcome the major drawback of the manual methods of selecting anatomical landmarks as alignment points. The results presented on *in vivo* radiographs show that the proposed geometric registration method produces smaller errors than the manual alignment method based on the projective transformation.

The proposed automatic geometric registration method is based on image's grey levels and is composed of a two-step process. Initially, the affine transformation parameters are calculated according to a multiresolution strategy and then a projective transformation is implemented at full resolution. The multiresolution approach has already been used for registering medical data from the same or different modalities and it has been shown that the application of a registration method from coarse-to-fine levels enhances the robustness of the registration.<sup>21–23</sup> In terms of

transformations used, the affine transformation is initially employed at the coarsest levels, as proposed by other researchers.<sup>5,10,13,14</sup> The affine transformation describes X-ray imaging with infinite distance between tube and subject, which causes the beams to be parallel. However, in intraoral radiography, parallelism in general is not preserved. Since the projective transformation perfectly describes X-ray imaging with an infinitely small focal spot size that equals an ideal point-source,<sup>7</sup> geometric registration of dental images based on projective geometry<sup>6,12,25</sup> has been proposed by several researchers. In the present paper, the initial registration using the affine transformation is refined by applying the projective transformation to the radiographs at full resolution. Furthermore, in the proposed geometric registration method, the normalized cross-correlation is employed as a similarity measure owing to its suitability for intramodal registration<sup>29</sup> and its

property of preventing the optimization technique to be trapped in local optima.

Another advantage of the proposed geometric registration method is its simplicity since it operates on the image's grey levels without any requirement for the application of a segmentation process prior to registration. In some approaches, the registration is based on the identification of edges of intrinsic features such as teeth or implants, the cemento-enamel junction or simply bony structures in the images to be registered.<sup>10,11,14</sup> The identification of common edge points is not always an easy task due to the presence of noise. Therefore, the performance of these approaches heavily depends on the accuracy of the segmentation method used. The developed automatic geometric registration method has been tested against the manual method widely used in a clinical setting. A number of corresponding point pairs greater than eight is considered, although four pairs are sufficient for the calculation of the projective transformation. Through this approach, the accuracy of the alignment via the manual registration method is improved. In a similar approach, it is stated that a number of landmarks greater than six improves the observer independence and the quality of the manual registration.<sup>12</sup>

The statistical analysis of the results listed in Table 1 has shown an advantageous performance of the proposed automatic registration method against the manual one for the majority of radiographic pairs in terms of the RMS error estimated over the whole images and specific ROIs. Furthermore, the manual method relies heavily on human intervention and depends on the number of corresponding points to compensate for interoperator variability. The number of landmarks placed determines the whole execution time. The execution time for the manual method including the placement of up to 16 point-pairs by an experienced dentist is more than 4 min. The average execution time for the proposed automatic registration method varies from 15 s to 50 s (AMD Athlon XP 1800). In a higher performance system, the execution time of the automatic registration method would significantly decrease while the execution time of the manual registration method would remain the same since it mainly depends on the time required for the careful placement of the landmarks with the algorithmic part being executed very fast.

## References

1. Gröndahl H-G, Gröndahl K, Webber RL. A digital subtraction technique for dental radiography. *Oral Surg Oral Med Oral Pathol* 1983; **55**: 96–102.
2. Gröndahl H-G, Gröndahl K. Subtraction radiography for the diagnosis of periodontal bone lesions. *Oral Surg Oral Med Oral Pathol* 1983; **55**: 208–213.
3. Brägger U. Radiographic parameters for the evaluation of peri-implant tissues. *Periodontology 2000* 1994; **4**: 87–97.
4. Benn DK. A review of the reliability of radiographic measurements in estimating alveolar bone changes. *J Clin Periodontol* 1990; **17**: 14–21.
5. Wenzel A, Hintze H. The choice of gold standard for evaluating tests for caries diagnosis. *Dentomaxillofac Radiol* 1999; **28**: 132–136.
6. Mol A, Dunn SM. The performance of projective standardization for digital subtraction radiography. *Oral Surg Oral Med Oral Pathol Oral Radiol Endod* 2003; **96**: 373–382.
7. Lehmann TM, Gröndahl H-G, Benn DK. Computer-based registration for digital subtraction in dental radiology. *Dentomaxillofac Radiol* 2000; **29**: 323–346.
8. Burdea G, Dunn SM, Levy G. Evaluation of robot-based registration for subtraction radiography. *Med Image Anal* 1999; **3**: 265–274.
9. Burdea G, Dunn SM, Mallik M, Immendorf C. Real time sensing of tooth position for dental digital subtraction radiography. *IEEE Trans Biomed Eng* 1991; **38**: 366–378.
10. Ellwood RP, Davies RM, Worthington HV. Evaluation of a dental subtraction radiography system. *J Periodont Res*. 1997; **32**: 241–248.
11. Ettinger GJ, Gordon GG, Goodson JM, Socransky SS, Williams R. Development of automated registration algorithms for subtraction radiography. *J Clin Periodontol* 1994; **21**: 540–543.

In addition to geometric registration, a universal contrast correction technique and fusion tools have been implemented for creating subtraction radiographs and fusion images. The contrast correction technique can be applied independently of the registration method employed and highlights differences of the progression/regression of a disease or the efficiency of a therapeutic scheme applied. The detection and quantification of early changes can be performed applying the subtraction radiographs. However, as unchanged structures are absent in noiseless subtraction radiographs, the location of areas with anatomical change is not depicted in relation to the stable structures. In cases where the visualization of the total anatomy is necessary, the fusion images can be used.

A general limitation of all geometric registration methods used for subtraction radiography, including the proposed automatic registration method, is the performance dependence of the projection errors upon acquisition of radiographs. In the present study, the implementation of the projective transformation model in both geometric registration methods under evaluation accounts for the minimization of reversible projection errors, as well recognized in the literature.<sup>6,12,25,30</sup> On the other hand, the performance and robustness of the registration methods in the presence of irreversible projection errors due to translations of the object, vertical and horizontal rotations of the object relative to the source and translations of the source, have been controlled only in *in vitro* studies where the image acquisition was standardized in terms of projection geometry.<sup>6,15</sup> It should be pointed out that *in vivo* material have been applied in order to test the performance of the registration methods, automatic and manual, in real clinical cases. Thus, the real displacements of the system components are not known. As a consequence, the limitations of the developed registration methods cannot be estimated. We assume that the proposed automatic registration method successfully aligns radiographs acquired under usual conditions (small projection errors in all degrees of freedom). A comparison of the two methods on a standardized acquisition environment in terms of projective geometry using *in vitro* material is planned for future investigation.

12. Lehmann TM, Gröndahl K, Gröndahl H-G, Schmitt W, Spitzer K. Observer-independent registration of perspective projection prior to subtraction of *in vivo* radiographs. *Dentomaxillofac Radiol* 1998; **27**: 140–150.
13. Byrd V, Mayfield-Donahoo T, Reddy MS, Jeffcoat MK. Semiautomated image registration for digital subtraction radiography. *Oral Surg Oral Med Oral Pathol Oral Radiol Endod* 1998; **85**: 473–478.
14. Yoon DC. A new method for the automated alignment of dental radiographs for digital subtraction radiography. *Dentomaxillofac Radiol* 2000; **29**: 11–19.
15. Gröndahl K, Gröndahl HG, Webber RL. Influence of variations in projection geometry on the detectability of periodontal bone lesions. *J Clin Periodontol* 1984; **11**: 411–420.
16. Gröndahl K, Gröndahl H-G, Wennström J, Heijl L. Examiner agreement in estimating changes in periodontal bone from conventional and subtraction radiographs. *J Clin Periodontol* 1987; **14**: 74–79.
17. Borg E, Gröndahl K, Persson LG, Gröndahl H-G. Marginal bone level around implants assessed in digital and film radiographs: *in vivo* study in the dog. *Clin Implant Dent Relat Res* 2000; **2**: 10–17.
18. Rosling B, Hollender L, Nyman S, Olsson G. A radiographic method for assessing changes in alveolar bone height following periodontal therapy. *J Clin Periodontol* 1975; **2**: 211–217.
19. Papika S, Paulsen HU, Shi XQ, Welander U, Linder-Aronson S. Orthodontic application of color image addition to visualize differences between sequential radiographs. *Am J Orthodont Dentofac Orthop* 1999; **115**: 488–493.
20. Ruttimann UE, Webber RL, Schmidt E. A robust digital method of film contrast correction in subtraction radiography. *J Periodont Res* 1986; **21**: 486–495.
21. Maes F, Vandermeulen D, Suetens P. Medical image registration using mutual information. *Proc IEEE* 2003; **91**: 1699–1722.
22. Thevenaz P, Unser M. Optimization of mutual information for multiresolution image registration. *IEEE Trans Image Proc* 2000; **9**: 2083–2099.
23. Maes F, Vandermeulen D, Suetens P. Comparative evaluation of multiresolution optimization strategies for multimodality image registration by maximization of mutual information. *Med Image Anal* 1999; **3**: 373–386.
24. Press W, Flannery B, Teukolsky S, Vetterling W. Numerical recipes in C. Cambridge: Cambridge University Press, 1992.
25. Ostuni J, Fisher E, van der Stelt PF, Dunn SM. Registration of dental radiographs using projective geometry. *Dentomaxillofac Radiol* 1993; **22**: 199–203.
26. Arun KS, Huang TS, Blostein S. Least-squares fitting of two 3-D point sets. *IEEE Trans PAMI* 1987; **9**: 698–700.
27. Gonzalez RC, Wintz P. Digital image processing. Reading MA: Addison-Wesley, 1977.
28. Bland JM, Altman DG. Statistical methods for assessing agreement between two methods of clinical measurement. *Lancet* 1986; **1**: 307–310.
29. Lehmann T, Sovakar A, Schmitt W, Repges R. A comparison of similarity measures for digital subtraction radiography. *Comput Biol Med* 1997; **27**: 151–167.
30. Fisher E, Van der Stelt PF, Ponce A, Fenesy K, Shaw S. A comparison of two registration techniques for digital subtraction radiography. *Dentomaxillofac Radiol* 1995; **24**: 5–12.